*Journal of Fluorescence, Vol. 15, No. 4, July 2005 (© 2005)*
DOI: 10.1007/s10895-005-2823-9

# Preparation, Characterization and Application of Fluorescent Terbium Complex-Doped Zirconia Nanoparticles

**Zhiqiang Ye,[1] Mingqian Tan,[1] Guilan Wang,[1] and Jingli Yuan[1,2]**

*Received December 9, 2004; accepted February 24, 2005*

Novel zirconia-based fluorescent terbium nanoparticles have been prepared as a fluorescent nanoprobe for time-resolved fluorescence bioassay. The nanoparticles were prepared in a water-in-oil (W/O) microemulsion consisting of a strongly fluorescent $Tb^{3+}$ complex, *N*,*N*,*N*$^1$,*N*$^1$-[2,6-*bis*(3′-aminomethyl-1′-pyrazolyl)-phenylpyridine]tetrakis(acetate)-$Tb^{3+}$(BPTA-$Tb^{3+}$), Triton X-100, hexanol, and cyclohexane by controlling co-condensation of $Zr(OCH_2CH_3)_4$ and $ZrOCl_2$. The characterizations by transmission electron microscopy and fluorometric methods indicate that the nanoparticles are uniform in size, $33 \pm 4$ nm in diameter, and have a fluorescence quantum yield of 8.9% and a long fluorescence lifetime of 2.0 ms. The zirconia-based fluorescent terbium nanoparticles show high stability against basic dissolution in a high pH aqueous buffer compared to the silica-based nanoparticles. A surface modification and bioconjugation method for the fluorescent nanoparticles was developed, and the nanoparticle-conjugated streptavidin (SA) was used for time-resolved floroimmunoassy (TR-FIA) of human prostate specific antigen (PSA). The result shows that the zirconia-based fluorescent terbium nanoparticles are useful as a fluorescent nanoprobe for time-resolved fluorescence bioassay.

**KEY WORDS:** Terbium complex; fluorescent nanoparticle; fluorescence probe; time-resolved fluoroimmunoassay.

## INTRODUCTION

Researches on the preparation, characterization and application of functionalized nanosized materials have increased tremendously during the last decade. Among these researches, fluorescent nanoparticles, offering effective signal amplification and high photostability compared to the conventional fluorescence dyes, have provided an attractive research field for biolabeling and biological detection. The representative fluorescent nanomaterials including quantum dots [1–4], plasmon-resonant nanoparticles [5], and luminophore-doped silica nanoparticles [7–9], have been explored as the luminescent nanoprobes for various bioassays. However, the luminescence *measurements* using these luminescent nanoprobes *are* easily affected by the strong non-specific background noises caused by the autofluorescence from biological samples, the scattering light associated with Tyndall, Rayleigh and Raman scatterings, and the luminescence from the optical components such as the cuvettes, filters and lenses. To resolve these problems, we recently developed several kinds of fluorescent lanthanide complex-doped silica nanoparticles as the fluorescent nanoprobes for biolabelings and time-resolved fluorescence bioassays [10–13]. These nanoparticles combined the advantages of both luminophore-doped silica nanoparticles and lanthanide fluorescence latexes including high hydrophilicity, photostability and biocompatibility have been expected to be *more useful* as fluorescence nanoprobes, since the fluorescence of the nanoparticles is long-lived, and the non-specific background noises can be easily eliminated by using time-resolved fluorescence measurement technique. *However, the use of a silica-based* fluorescent nanoprobe for bioassay has a problem that the silica network of

[1] Department of Analytical Chemistry, Dalian Institute of Chemical Physics, Chinese Academy of Sciences, Dalian 116023, Peoples' Republic of China.
[2] To whom correspondence should be addressed E-mail: jingliyuan@yahoo.com.cn

the nanoparticles might be dissolved in a basic aqueous medium [14].

Zirconia is an important ceramic material and has been applied as a functional material in a number of technologies, such as high performance liquid chromatography [15–18], catalyst [19], oxygen sensor [20], damage resistant optical coating [21], buffer layer for superconductor growth [22], and gate dielectric [23]. Compared with silica material, zirconia material has better resistance against dissolution in high pH buffers and stronger ability to tolerate organic solvents, high temperatures and pressures [16]. Several methods have been investigated for the preparation of zirconia nanoparticles including sol–gel process [24], spray pyrolysis [25], salt-assisted aerosol decomposition [26], and emulsion precipitation [27]. However, the nanoparticles prepared by these methods *showed the* broad particle size distributions, and *a* successful preparation method of uniform-sized and luminophore-doped zirconia nanoparticles has not been reported.

In the present work, novel fluorescent terbium complex-doped zirconia nanoparticles with uniform size and strong fluorescence were prepared using a water-in-oil microemulsion technique by controlling the co-condensation of $ZrOCl_2$ and $Zr(OCH_2CH_3)_4$. A strongly fluorescent $Tb^{3+}$ complex, *N*,*N*,*N*$^1$,*N*$^1$-[2,6-*bis*(3′-aminomethyl-1′-pyrazolyl)-4-phenylpyridine] tetrakis(acetate)-$Tb^{3+}$ (BPTA-$Tb^{3+}$), was doped inside zirconia network of the nanoparticles. The zirconia matrix of the nanoparticles not only shows high stability in *a* strong basic solution, its surface can directly attach biomolecules due to the presence of the unsaturated coordinative zirconium(IV) sites. After the *nanoparticles were* coated with bovine serum albumin (BSA) by physical absorption, the *BSA-coated* nanoparticles were covalently bound to streptavidin (SA). The result of time-resolved fluoroimmunoassay (TR-FIA) for human prostate specific antigen (PSA) using the nanoparticle-conjugated SA reveals that the fluorescent terbium complex-doped zirconia nanoparticles are a useful fluorescent nanoprobe for time-resolved fluorescence bioassay.

## EXPERIMENTAL

### Materials and Physical Measurements

The BPTA-$Tb^{3+}$ complex was synthesized by using a previous method [28]. $ZrOCl_2$, $Zr(OCH_2CH_3)_4$ and Triton X-100 were purchased from Acros Organics. SA was purchased from Chemicon International Inc. Mouse monoclonal and goat polyclonal anti-human PSA antibodies were purchased from OEM Concepts Co. Sulfosuccinimidyl-6-(biotin-amido)hexanoate (NHS-LC-biotin) was purchased from Pierce Chemical Co. The standard solutions of human PSA were prepared by diluting human PSA antigen (Biogenesis Ltd.) with 0.05 M Tris–HCl buffer of pH 7.8 containing 5% BSA, 0.9% NaCl and 0.1% $NaN_3$.

A JEOL model JEM-2000EX transmission electron microscope was used for measuring the shape and size of the nanoparticles. X-ray diffraction (XRD) spectrum was measured on a Rigaku diffractometer (D/Max-$\gamma$B, Japan). The X-ray diffraction pattern was recorded from 5 to 60° ($2\theta$ value) using CuK$\alpha$ radiation, and a generator voltage of 40 kV and a current of 70 mA. Thermogravimetry (TG) and differential scanning calorimeter (DSC) analyses were carried out on a Mettler Toledo TGA/SDTA851–thermoanalyzer (Swiss, $N_2$ atmosphere, 50 ml/min, heating rate 10 K/min) and a TA Instruments model 910S differential scanning calorimeter (USA, $N_2$ atmosphere, 200 ml/min, heating rate 10 K/min), respectively. Fluorescence spectra and emission lifetime were measured on a Perkin Elmer LS 50B spectrofluorometer. The TR-FIA was carried out with FluoroNunc 96-well microtiter plate as the solid-phase carrier and measured on a Perkin–Elmer Victor 1420 multilabel counter with the conditions of excitation wavelength, 320 nm, emission wavelength, 545 nm, delay time, 0.2 ms, and window time, 0.4 ms.

### Preparation of Nanoparticles

A W/O microemulsion consisting of 2.38 g Triton X-100, 1.88 g hexanol, 7.25 g cyclohexane, 0.4 ml ethanol solution of 0.01 mg $Zr(OC_2H_5)_4$, 1.5 ml aqueous solution of 10 mg BPTA-$Tb^{3+}$ and 0.03 mg $ZrOCl_2$ was mixed with a W/O microemulsion consisting of 0.17 g Triton X-100, 0.13 g hexanol, 0.52 g cyclohexane and 14 $\mu$l concentrated ammonia water with vigorous stirring. After stirring for 48 h, the precipitate was obtained by adding acetone, centrifuging, and washing with ethanol and water for several times to remove surfactant and unreacted materials. The pale yellow $Tb^{3+}$ complex-doped fluorescent zirconia nanoparticles were obtained by drying the precipitate in desiccator for 1 day and in electrothermal stove at 250°C for 1 h.

### Preparation of the Nanoparticle-Conjugated SA

After the nanoparticles (2.0 mg) and BSA (10 mg) suspended in 1.0 ml of 0.1 M phosphate buffer of pH 7.0 were stirred for 24 h at room temperature, the BSA-coated nanoparticles were centrifuged and washed with phosphate buffer and water. The BSA-coated nanoparticles

were suspended in 1.0 ml of 0.1 M phosphate buffer of pH 7.0 again, and then 1.0 mg of SA and 0.1 ml of 1% glutaraldehyde were added. After the suspension was stirred at 4°C for 24 h, 2 mg of $NaBH_4$ was added. The suspension was further incubated at room temperature for 2 h. The nanoparticle-conjugated SA was centrifuged, washed with phosphate buffer and water, and diluted with 0.05 M Tris–HCl buffer of pH 7.8 containing 0.2% BSA, 0.1% $NaN_3$ and 0.9% NaCl, and than stored at 4°C.

### Preparation of Biotinylated Goat Anti-Human PSA Antibody

After two dialyses of 1.0 ml goat anti-human PSA antibody solution (0.5 mg/ml) for 24 h at 4°C against 3 L of saline water, 8.4 mg $NaHCO_3$ and 3 mg NHS-LC-biotin were added. After stirring for 1 h at room temperature, the solution was further incubated for 24 h at 4°C. The solution was twice dialyzed each for 24 h at 4°C against 3 L of 0.1 M $NaHCO_3$ containing 0.25 g $NaN_3$, then 5 mg BSA and 5 mg $NaN_3$ were added. The solution was stored at −20°C before use. When the biotinylated antibody solution was used for immunoassay, it was diluted 300-fold with 0.05 M Tris–HCl buffer of pH 7.8 containing 0.2% BSA, 0.9% NaCl and 0.1% $NaN_3$.

### Immunoassay of Human PSA Using the Nanoparticle-Conjugated SA

After anti-human PSA monoclonal antibody (diluted to 10 $\mu$g/ml with 0.1 M carbonate buffer of pH 9.6) was coated on the wells (50 $\mu$l per well) of a 96-well microtiter plate by physical adsorption [29], 45 $\mu$l of human PSA standard solution was added to each well. The plate was incubated at 37°C for 1 h, and washed with 0.05 M Tris–HCl buffer of pH 7.8 containing 0.05% Tween 20 and 0.05 M Tris–HCl buffer of pH 7.8. Then the biotinylated antibody (∼1.1 $\mu$g/ml, 45 $\mu$l per well) was added to each well, and the plate was incubated at 37°C for 1 h. After washing, the nanoparticle-conjugated SA (∼20 $\mu$g/ml, 45 $\mu$l per well) was added to each well, and the plate was incubated at 37°C for 1 h. The plate was washed four times with 0.05 M Tris–HCl buffer of pH 7.8 containing 0.05% Tween 20, and subjected to solid-phase time-resolved fluorometric measurement.

## RESULTS AND DISCUSSION

The preparations of various nanoparticles were generally performed in heterogeneous media, such as emulsion and microemulsion, using the interior dispersed aqueous phase as isolated nanoreactors to obtain non-agglomerated nanoparticles [30]. In the present work, the fluorescent terbium complex-doped zirconia nanoparticles were prepared in a W/O microemulsion containing aqueous solution of BPTA-$Tb^{3+}$, surfactant Triton X-100, cosurfactant hexanol, and oil-phase cyclohexane by hydrolysis co-condensation of $ZrOCl_2$ and $Zr(OCH_2CH_3)_4$. The drying process of the nanoparticles at 250°C enables the adhesive water molecules in the nanoparticles to be effectively removed. The transmission electron microscopy (TEM) image and particle size histogram of the nanoparticles (Fig. 1) indicate that the zirconia nanoparticles prepared by this method are monodisperse, spherical and uniform in size, 33 ± 4 nm in diameter.

Thermogravimetry (TG) and differential scanning calorimeter (DSC) analyses were used for evaluating the thermal stability of BPTA-$Tb^{3+}$ complex (Fig. 2). The mass loss between ∼50–200°C with a broad endothermic peak is caused by the release of crystal water in the complex, and the exothermic peak at ∼360°C is caused by the decomposition of BPTA-$Tb^{3+}$ complex. This result shows that the BPTA-$Tb^{3+}$ complex is stable below 300°C, and the drying process of the nanoparticles in electrothermal stove at 250°C does not decompose the fluorescent $Tb^{3+}$ complex. The X-ray diffraction (XRD) spectrum of the nanoparticles is shown in Fig. 3. The zirconia-based fluorescent nanoparticles do not show any sharp diffraction peaks, which indicates the nanoparticles are an amourphous or ultrasmall crystalline material [11].

The time-resolved fluorescence spectra of the nanoparticles and pure BPTA-$Tb^{3+}$ complex measured in 0.1 M phosphate buffer of pH 7.1 were shown in Fig. 4. Both BPTA-$Tb^{3+}$ complex and the nanoparticles show the same spectrum patterns with the excitation and emission maximum wavelengths at 324 and 543 nm, respectively. The fluorescence quantum yield of the nanoparticles in 0.05 M borate buffer of pH 9.1 was measured to be 8.9% (the experimental uncertainty <15%) by using a reported method [31] and calculated using the equation of $\phi_1 = I_1 A_2 \phi_2 / I_2 A_1$ with a standard quantum yield [32] of $\phi_2 = 10.0\%$ for a $Tb^{3+}$ chelate of *N*,*N*,$N^1$,$N^1$-[4′-phenyl-2,2′:6′,2″-terpyridine-6,6″-diyl] *bis*(methylenenitrilo)tetrakis(acetate). In the equation, $I_1$ and $I_2$ are the fluorescence intensities of the nanoparticles and the standard, and $A_1$ and $A_2$ are the optical densities of the nanoparticles and the standard, respectively. The fluorescence lifetime of the nanoparticles was measured to be 2.0 ms. These results indicate that the fluorescent terbium chelate-doped zirconia nanoparticles prepared in this work have good fluorescence properties for time-resolved fluorometric application.

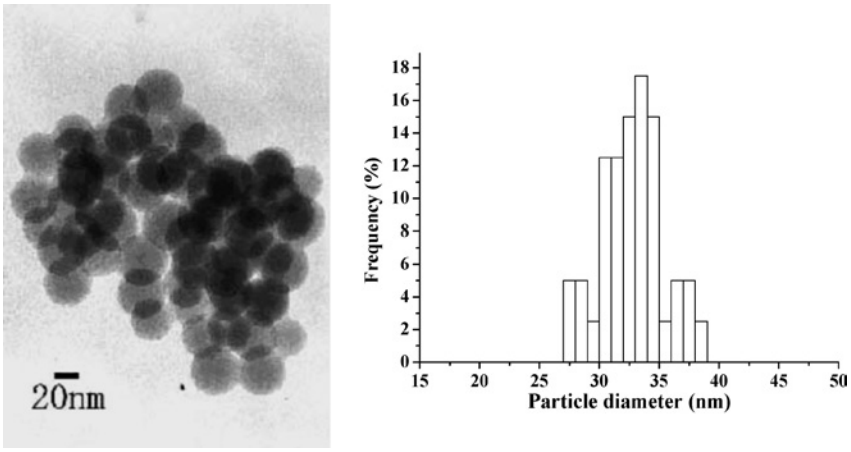


**Fig. 1.** TEM image (at ×250,000 magnification) and size histogram of the $Tb^{3+}$ complex-doped zirconia nanoparticles.

To evaluate the stability of zirconia matrix in a high pH aqueous medium, the BPTA-$Tb^{3+}$-doped zirconia nanoparticles and silica nanoparticles (prepared using a previous method [10]) were added to 1.0 M $Na_2CO_3$ solution with stirring, respectively. Each for 1 h, a portion of 1.0 ml solution was centrifuged. The precipitate was washed twice with water, redispersed in 1.0 ml of water, and then the fluorescent intensity was measured. The experiment was carried out for a period of 18 h. As shown in Fig. 5, after 18 h, the fluorescence intensity of the zirconia-based nanoparticles decreased only less than 3%, whereas that of the silica-based nanoparticles was decreased approximately by 60%. The fluorescence intensity decrease of the BPTA-$Tb^{3+}$-doped silica nanoparticles is caused by the dissolution of silica in 1.0 M $Na_2CO_3$ solution, which releases the fluorescent $Tb^{3+}$ complex molecules in silica nanoparticles into the $Na_2CO_3$ solution. These results indicate that zirconia matrix is highly stable in high pH aqueous solution and zirconia-based fluorescent nanoparticles can be used in a *broader* pH range compared to silica-based nanoparticles.

Zirconia-based nanoparticles can be conjugated with proteins easily due to the presence of unsaturated zirconium coordinative sites on their surface [33–35].

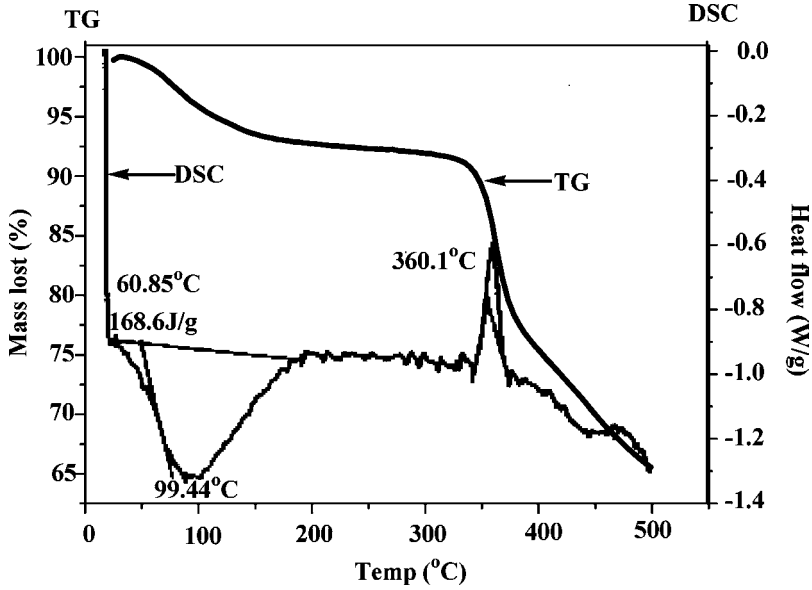


**Fig. 2.** Curves of TG and DSC analyses of the BPTA-$Tb^{3+}$ complex.

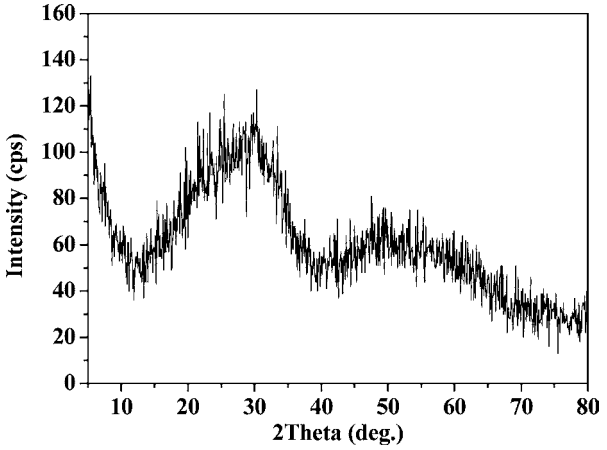


**Fig. 3.** XRD spectrum of the $Tb^{3+}$ complex-doped zirconia nanoparticles.

These sites account for the strong and hard Lewis acidity [36,37], and have a great affinity with hard Lewis bases, such as carboxylate and amino groups in protein molecules. Therefore zirconia-based nanoparticles can form stable complexes with protein molecules by the formation of Lewis acid-base pairs on the nanoparticle's surface. Based on this property, a method for the surface modification and bioconjugation of the BPTA-$Tb^{3+}$-doped zirconia nanoparticles was developed. As shown in Fig. 6, after nanoparticle's surface was coated with BSA by Lewis acid–base reaction, the BSA-coated

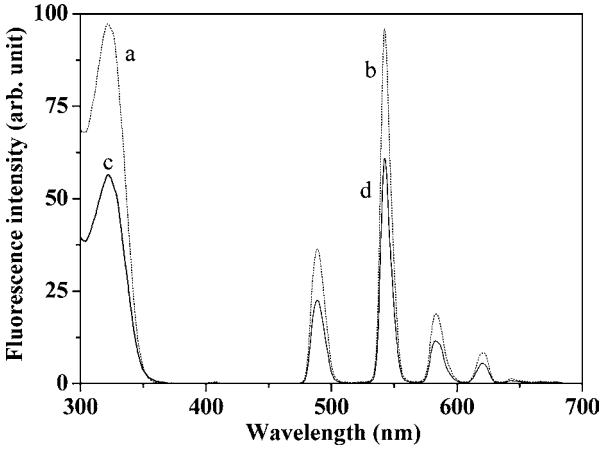


**Fig. 4.** Time-resolved fluorescence excitation and emission spectra of pure BPTA-$Tb^{3+}$ complex (0.33 $\mu$M, a, b) and the $Tb^{3+}$ complex-doped zirconia nanoparticles (3.3 mg/L, c, d) in 0.1 M phosphate buffer of pH 7.1. The conditions of delay time, 0.2 ms, gate time, 0.4 ms, cycle time, 20 ms, excitation slit, 10 nm, and emission slit, 5 nm, were used for the measurements. Excitation spectra were recorded with $\lambda_{em} = 543$ nm and emission spectra with $\lambda_{ex} = 324$ nm.

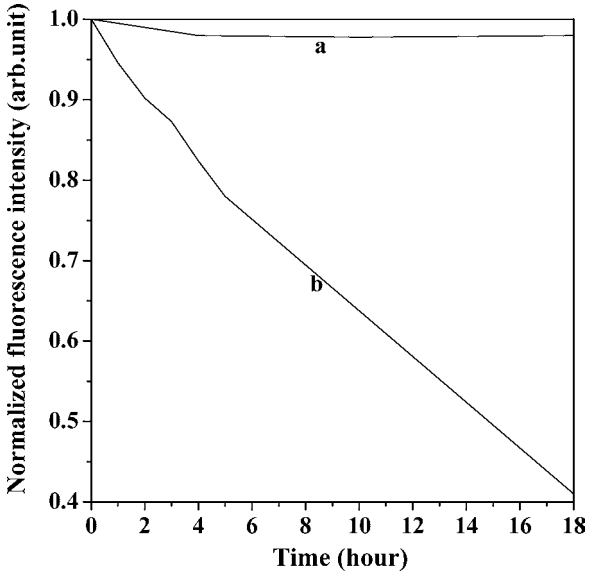


**Fig. 5.** Stability experiments: (a) the BPTA-$Tb^{3+}$ complex-doped zirconia nanoparticles; (b), the BPTA-$Tb^{3+}$ complex-doped silica nanoparticles, in 1.0 M $Na_2CO_3$ solution.

nanoparticles were further conjugated to SA by coupling the amino groups of BSA and SA with glutaraldehyde [38]. The role of $NaBH_4$ used in the labeling process is to reduce the N═C double bond (Shiff base) formed by the condensation reaction of the amino groups of BSA and SA with glutaraldehyde to a more stable N—C single bond. The BSA 'bridge' between the nanoparticle and SA has the function to reduce the effect of the nanoparticles on the bioactivity of SA.

The TR-FIA of human PSA was used to evaluate the usefulness of the zirconia nanoparticles as a fluorescent probe for time-resolved fluorescence *bioassay*. Figure 7 shows the calibration curve for PSA detection. The detection limit, defined as the concentration corresponding to 3SD (standard deviation) of background signal, is 0.4 ng/ml. The dynamic range is up to ~10 ng/ml. Compared with the TR-FIA of human PSA using the BPTA-$Tb^{3\pm}$ complex-doped silica nanoparticles [10], the detection limit of the present method is obviously high. This would be caused by the preparation method of the nanoparticle-conjugated SA. Even though the Lewis acid–base conjugation of zirconia nanoparticle-BSA is relatively stable, it would be possible that the conjugation dissociates at lower concentration or in the washing processes of the assay, which causes some fluorescent nanoparticles to be lost, and results in the decrease of the detection sensitivity. However, the present primary results still indicate that the fluorescent zirconia nanoparticles are useful as a fluorescent nanoprobe for biolabeling and time-resolved fluorescence bioassay.

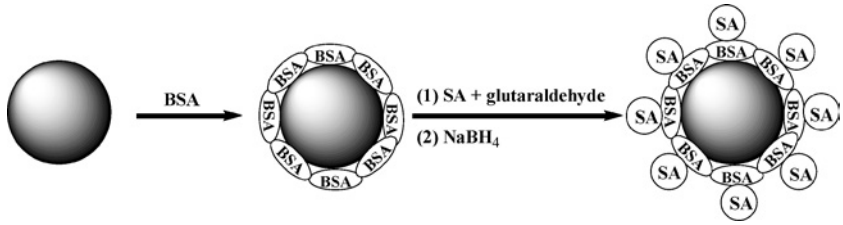


**Fig. 6.** Immobilization processes of SA onto the $Tb^{3+}$ complex-doped zirconia nanoparticles.

## CONCLUSIONS

Uniform terbium complex-doped fluorescent zirconia nanoparticles having small size, relatively strong fluorescence and long fluorescence lifetime were prepared, characterized and developed as a fluorescent nanoprobe for biolabling and time-resolved fluorescence bioassay. The nanoparticles are highly stable in high pH media compared to the silica-based nanoparticles, which makes the zirconia-based fluorescent nanoparticles suitable be used for the assay that higher pH buffers have to be used. The applications of the nanoaprticles for bioconjugation and TR-FIA show that the nanoparticles are a useful fluorescent nanoprobe even though further improvement is necessary. It can be expected that the new fluorescent nanoparticles would be widely useful in time-resolved fluorescence biotechnologies, such as immunoassay, bioimaging microscopy and biochip technologies .

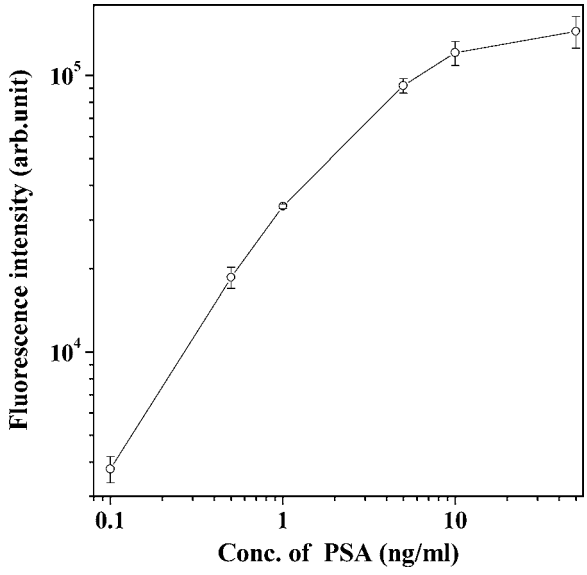


**Fig. 7.** Calibration curve of TR-FIA useing the $Tb^{3+}$ complex-doped zirconia nanoparticle-conjugated SA for human PSA.

## ACKNOWLEDGMENTS

The authors thank for the support from The National Natural Science Foundation of China (20175027) and Scientific Research Innovation Foundation of the Chinese Academy of Sciences.

## REFERENCES

1. M. Bruchez, Jr., M. Moronne, P. Gin, S. Weiss, and A. P. Alivisatos (1998). Semiconductor nanocrystals as fluorescent biological labels. *Science* **281**, 2013–2016.
2. W. C. W. Chan and S. Nie (1998). Quantum dot bioconjugates for ultrasensitive nonisotopic detection. *Science* **281**, 2016–2018.
3. J. R. Taylor, M. M. Fang, and S. Nie (2000). Probing specific sequences on single DNA molecules with bioconjugated fluorescent nanoparticles. *Anal. Chem.* **72**, 1979–1986.
4. G. P. Mitchell, C. A. Mirkin, and R. L. Letsinger (1999). Programmed assembly of DNA functionalized quantum dots. *J. Am. Chem. Soc.* **121,** 8122–8123.
5. S. Schultz, D. R. Smith, J. J. Mock, and D. A. Schultz (2000). Single-target molecule detection with nonbleaching multicolor optical immunolabels. *Proc. Natl. Acad. Sci. U.S.A.* **97**, 996–1001.
6. M. A. Hayat (1989). *Colloidal Gold: Principles, Methods and Applications,* Academic Press, New York.
7. S. Santra, P. Zhang, K. Wang, R. Tapec, and W. Tan (2001). Conjugation of biomolecules with luminophore-doped silica nanoparticles for photostable biomarkers. *Anal. Chem.* **73**, 4988–4993.
8. X. Zhao, R. T. Dytioco, and W. Tan (2003). Ultrasensitive DNA detection using highly fluorescent bioconjugated nanoparticles. *J. Am. Chem. Soc.* **125**, 11474–11475.
9. X. Zhao, L. R. Hilliard, S. J. Mechery, Y. Wang, P. P. Bagwe, S. Jin, and W. Tan (2004). A rapid bioassay for single bacterial cell quantitation using bioconjugated nanoparticles. *Proc. Natl. Acad. Sci. U.S.A.* **101**, 15027–15032.
10. Z. Ye, M. Tan, G. Wang, and J. Yuan (2004). Preparation, characterization and time-resolved fluorometric application of silica-coated terbium(III) fluorescent nanoparticles. *Anal. Chem.* **76**, 513–518.
11. M. Tan, Z. Ye, G. Wang, and J. Yuan (2004). Preparation and time-resolved fluorometric application of the luminescent europium nanoparticles. *Chem. Mater.* **16**, 2494–2498.
12. M. Tan, G. Wang, X. Hai, Z. Ye, and J. Yuan (2004). Development of functionalized fluorescent europium nanoparticles for biolabeling and time-resolved fluorometric application *J. Mater. Chem.* **14**, 2896–2901.
13. Z. Ye, M. Tan, G. Wang, and J. Yuan (2005). Development of functionalized terbium fluorescence nanoparticles for antibody labeling and time-resolved fluoroimmunoassay application. *Talanta* **65**, 206–210.
14. H. Poppe (1997). Some reflections on speed and efficiency of modern chromatographic methods. *J. Chromatogr. A* **778**, 3–21.

15. H. J. Wirth and M. T. W. Hearn (1993). High-performance liquid chromatography of amino acids, peptides and proteins. *J. Chromatogr.* **646**, 143–151.
16. A. M. Clausen and P. W. Carr (1998). Chromatographic characterization of phosphonate analog EDTA-modified zirconia support for biochromatographic applications. *Anal. Chem.* **70**, 378–385.
17. A. M. Clausen, A. Subramanian, and P. W. Carr (1999). Purification of monoclonal antibodies from cell culture supernatants using a modified zirconia based cation-exchange support. *J. Chromatogr. A* **831**, 63–72.
18. H. J. Wirth and M. T. W. Hearn (1995). Adsorbents for the removal of humic acid from surface water based on modified porous zirconia and silica. *J. Chromatogr. A* **711**, 223–233.
19. J. F. Haw, J. Zhang, K. Shimizu, T. N. Venkatraman, D. P. Luigi, W Song, D. H. Barich, and J. B. Nicholas (2000). NMR and theoretical study of acidity probes on sulfated zirconia catalysts. *J. Am. Chem. Soc.* **122**, 12561–12570.
20. C. León, M. L. Lucía, and J. Santamaría (1997). Correlated ion hopping in single-crystal yttria-stabilized zirconia. *Phys. Rev. B* **55**, 882–887.
21. N. Mansour, K. Mansour, E. W. V. Stryland, and M. J. Soileau (1990). Diffusion of color centers generated by two-photon absorption at 532 nm in cubic zirconia. *J. Appl. Phys.* **67**, 1475–1477.
22. J. M. Phillips (1996). Substrate selection for high-temperature superconducting thin films. *J. Appl. Phys.* **79**, 1829–1848.
23. G. D. Wilk, R. M. Wallace, and J. M. Anthony (2001). High-kappa gate dielectrics: Current status and materials properties considerations. *J. Appl. Phys.* **89**, 5243–5275.
24. Y. T. Moon, H. K. Park, D. K. Kim, and C. H. Kim (1995). Preparation of monodisperse and spherical zirconia powders by heating of alcohol-aqueous salt-solutions. *J. Am. Ceram. Soc.* **78**, 2690–2694.
25. W. Stichert and F. Schüth (1998). Influence of crystallite size on the properties of zirconia. *Chem. Mater.* **10**, 2020–2026.
26. B. Xia, I. W. Lenggoro, and K. Okuyama (2001). Novel route to nanoparticle synthesis by salt-assisted aerosol decomposition. *Adv. Mater.* **13**, 1579–1579.
27. F. C. M. Woudenberg, W, F. C. Sager, N. G. M. Sibelt, and H. Verweij (2001). Dense nanostructured t-$ZrO_2$ coatings at low temperatures via modified emulsion precipitation. *Adv. Mater.* **13**, 514–516.
28. J. Yuan, G. Wang, K. Majima, and K. Matsumoto (2001). Synthesis of a terbium fluorescent chelate and its application to time-resolved fluoroimmunoassay. *Anal. Chem.* **73**, 1869–1876.
29. K. Matsumoto, J. Yuan, G. Wang, and H. Kimura (1999). Simultaneous determination of d-fetoprotein and carcinoembryonic antigen in human serum by time-resolved fluoroimmunoassay. *Anal. Biochem.* **276**, 81–87.
30. J. Wang, L. S. Ee, S. C. Ng, C. H. Chew, and L. M. Gan (1997). Reduced crystallization temperature in a microemulsion-derived zirconia precursor. *Mater. Lett.* **30**, 119–124.
31. L. Qu and X. Peng (2002). Control of photoluminescence properties of CdSe nanocrystals in growth. *J. Am. Chem. Soc.* **124**, 2049–2055.
32. M. Latva, H. Takalo, V.-M. Mukkala, C. Matachescu, J. C. Rodríguez-Ubis, and J. Kankare (1997). Correlation between the lowest triplet state energy level of the ligand and lanthanide(III) luminescence quantum yield. *J. Luminesc.* **75**, 149–169.
33. K. K. Unger and U. Trüdinger (1989). Qualitative supercritical fluid chromatography/fourier transform infrared spectroscopy study of methylene chloride and supercritical carbon dioxide extracts of double-base propellant. *Anal. Chem.* **61**, 145–148.
34. A. A. Tsyganenko and V. N. Filimonov (1972). Infrared spectra of surface hydroxyl groups and crystalline structure of oxides. *Spectrosc. Lett.* **5**, 477–483.
35. J. A. Blackwell and P. W. Carr (1992). Ion-exchange and ligand-exchange chromatography of proteins using porous zirconium-oxide supports in organic and inorganic lewis base eluents. *J. Chromatogr.* **596**, 27–41.
36. R. E. Connick and W. H. Mcvey (1949). The aqueous chemistry of zirconium. *J. Am. Chem. Soc.* **71**, 3182–3191.
37. A. J. Zielen and R. E. Connick (1956). Investigation of the complexes of mercury(II) with ethylenediaminetetraacetic acid using the mercury electrode. *J. Am. Chem. Soc.* **78**, 5785–5792.
38. J. Yuan, G. Wang, H. Kimura, and K. Matsumoto (1997). Highly sensitive time-resolved fluoroimmunoassay of human immunoglobulin E by using a new europium fluorescent chelate as a label. *Anal. Biochem.* **254**, 283–287.